RESEARCH PAPER

Bis Sulfamic Acid Functionalized Magnetic Nanoparticles as a Retrievable Nanocatalyst for the Green Synthesis of Polyhydroquinolines and Tetrahydrobenzopyrans

Mohammad Ali Bodaghifard[1,2]*

[1] *Department of Chemistry, Faculty of Science, Arak University, Arak, Iran*

[2] *Institute of Nanosciences and Nanotechnolgy, Arak University, Arak, Iran*

ARTICLE INFO

Article History:
Received 14 October 2018
Accepted 08 December 2018
Published 01 January 2019

Keywords:
Green Chemistry
Hybrid Nanoparticles
Polyhydroquinoline
Sulfamic Acid
Tetrahydrobenzopyran

ABSTRACT

Synthesis of bis sulfamic acid-grafted on silica-coated nano-Fe3O4 particles (MNPs-TBSA) as a novel core/shell hybrid organic-inorganic magnetic nanostructures, and their performance as a retrievable heterogeneous acidic catalyst is disclosed. The catalytic performance of this novel material was studied for the green synthesis of pharmaceutically valuable polyhydroquinoline and tetrahydrobenzopyran derivatives via one-pot multi-component condensation of aryl aldehydes, dimedone, ethyl acetoacetate, malononitrile and ammonium actate in ethanol as a solvent and at 70 ° C. Eco-friendly method, high yield and purity of the desired products, short reaction time along with the ease of the workup procedure outlines the advantages of these new methodologies over the earlier ones. Surface and magnetic properties of the core/shell hybrid nanoparticles were characterized via field emission scanning electron microscopy (FE-SEM), X-ray diffraction measurements (XRD), the energy dispersive X-ray spectroscopy (EDS), FT-IR spectroscopy and vibrating sample magnetometer (VSM). The crystallite size of the magnetic nanoparticle is calculated to be 15.5 nm.

How to cite this article
Bodaghifard MA. Bis Sulfamic Acid Functionalized Magnetic Nanoparticles as a Retrievable Nanocatalyst for the Green Synthesis of Polyhydroquinolines and Tetrahydrobenzopyrans. J Nanostruct, 2019; 9(1): 29-40. DOI: 10.22052/JNS.2019.01.005

INTRODUCTION

1,4-Dihydropyridyl compounds (1,4-DHPs) are valuable heterocyclic compounds in view of pharmaceuticals and drugs development [1]. 1,4-DHPs possess a wide range of biological activities such as anti-atherosclerotic, vasodilator, anti-diabetic, geroprotective, hepatoprotective and the treatment of hypertention and cardiovascular diseases [2-6]. 4*H*-Pyran compounds present a broad range of biological and pharmacological properties such as anticancer, anti-HIV, anti-inflammatory, anti-microbial, anti-malarial, anti-hyperglycaemic and anti-dyslipidemic activity [7-13]. Realizing the importance of 1,4-dihydropyridyl compounds and 4H-pyran derivatives, increasing interest on synthetic methods of these compounds is ongoing. The classical method for polyhydroquinoline synthesis involves a three-component coupling of an aldehyde, dicarbonyl compounds, and ammonia in acetic acid or in refluxing ethanol for long reaction times which typically leads to low yields [14-16]. Traditional processes for 4*H*-pyran synthesis were reported as the reaction of active methylene compounds with an aldehyde or ketone in the presence of an organic base such as piperidine or triethylamine under reflux and multiple-step conditions [17]. In recent years, several modified synthesis methods to access polyhydroquinolines [18-28], and 4*H*-benzo[*b*]pyrans [29-36], have been developed. Although some reactions are satisfactory in terms

* *Corresponding Author Email: mbodaghi2007@yahoo.com*
m-bodaghifard@araku.ac.ir

of yield, but the use of high temperatures, expensive metal precursors, catalysts that are harmful to the environment, long reaction times, harsh reaction conditions, effluent pollution and tedious workup procedures are drawbacks of these methods.

Nanotechnology is beginning to allow scientists, engineers, chemists, and physicians to work at the molecular and cellular levels to produce important advances in the life sciences and healthcare. The uses of synthetic nanomaterials have increased the scope of their application in areas of medical diagnostics, areas of material modification, degradation of environmental pollutants, chemical reaction catalysis and biotechnology [37, 38]. These widespread applications results to the necessity of nanomaterials modification into different structure with desirable features.

Organic-inorganic hybrid materials are of great interest as heterogeneous catalysts in organic synthesis, due to the functional diversity merged with thermal and mechanical stability of inorganic solids [39]. Their large surface area per unit volume, makes them interesting in the heterogeneous catalysis area; Heterogeneous catalysis in the nano-scale takes advantage of a high exposure of the active species leading to a higher efficiency of the catalyst [40]. Nevertheless, the application of heterogeneous nanocatalysts are usually limited by the inevitable loss of catalyst during the tedious separation processes, i.e. filtration or centrifugation. In this vein, easily separable magnetic nanoparticles (MNPs), e.g. Fe_3O_4, have demonstrated high stability, easy synthesis and functionalization alongside with high surface area, low toxicity and cost. These superb properties set magnetic nanoparticles as a target for extensive investigation as inorganic supports in the synthesis of semi-heterogeneous catalysts [41]. These metallic nanoparticles can be coated with silica shell to introduce numerous surface Si–OH groups for further modification and higher chemical and colloidal stability since the magnetically agglomeration will be diminished [42].

For the above reasons and as a part of our works on design and development of novel heterogeneous catalysts and green chemical methods [43-47], we describe the synthesis and characterization of bis-sulfamic acid-grafted magnetic nanoparticles (MNPs-TBSA) to give access to biologically interesting polyhydroquinolines and 4*H*-benzo[*b*] pyrans as a new eco-friendly method (Fig. 1). This novel designed catalyst provided a heterogeneous system with a green synthetic aspects by avoiding the use of hazardous conditions for accessing target heterocyclic compounds.

MATERIALS AND METHODS

All chemicals were purchased from Merck or Acros chemical companies and used without further purification. Melting points were measured by using capillary tubes on an electro

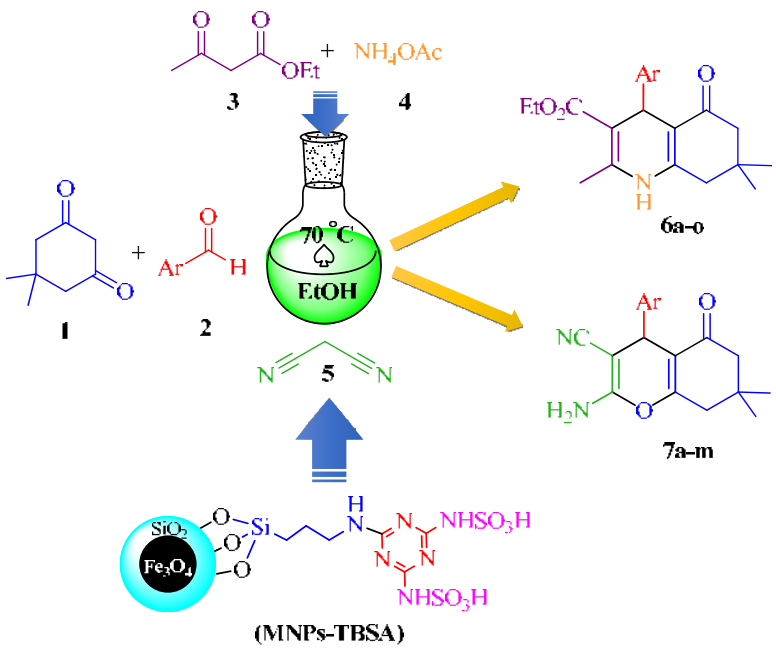

Fig. 1. Synthesis of polyhydroquinoline and 4*H*-benzo[*b*]pyran derivatives in the presence of MNPs-TBSA as a catalyst

thermal digital apparatus and are uncorrected. Known products were identified by comparison of their spectral data and melting points with those reported in the literature. Thin layer chromatography (TLC) was performed on UV active aluminum backed plates of silica gel (TLC Silica gel 60 F254). ^{1}H and ^{13}C NMR spectra were recorded on a Bruker Avance 300 MHz spectrometer at 300 MHz and 75 MHz, respectively. Coupling constants, J, were reported in hertz unit (Hz). IR spectra were recorded on a Unicom Galaxy Series FT-IR 5030 spectrophotometer using KBr pellets and are expressed in cm^{-1}. Elemental analyses were performed by Vario EL equipment at Arak University. X-ray diffraction (XRD) was performed on Philips XPert (Cu-K_{α} radiation, λ = 0.15405 nm) over the range 2θ = 20-80° using 0.04° as the step length. Thermal gravimetric analysis (TGA) and differential thermal gravimetric (DTG) data for MNPs-TBSA were recorded on a Mettler TA4000 System under an N_2 atmosphere at a heating rate of 10 °C min^{-1}. The scanning electron microscope measurement was carried out on a Hitachi S-4700 field emission-scanning electron microscope (FE-SEM).

General procedure for the synthesis of polyhydroquinolines

A mixture of dimedone (1 mmol), ethylaceto-acetate (1 mmol), aldehyde (1 mmol), ammonium acetate (1.2 mmol) and MNPs-TBSA (30 mg) as catalyst in 5 mL EtOH was heated at 70 °C and were stirred for appropriate time. After completion of the reaction as followed by TLC, the resulting solidified mixture was diluted with hot EtOH (15 mL). Then, the catalyst was separated using an external magnet, the solvent was evaporated, and the product was recrystallized with EtOH/H_2O (4:1), and dried in an oven at 90 °C (Table 2).

General procedure for the synthesis of 4H-benzo[b] pyrans

A mixture of an aromatic aldehyde (1 mmol), malononitrile (1 mmol), dimedone (1 mmol) and MNPs-TBSA (30 mg) as catalyst in 5 ml EtOH was heated at 70 °C with stirring for an appropriate time. The resulting solidified mixture was diluted with hot EtOH (15 mL). Then, the catalyst was separated using an external magnet, the solvent was evaporated, and the product was recrystallized with EtOH/H_2O (4:1), and dried in an oven at 90 °C (Table 4).

Selected data for desired products

6a: IR (KBr) (ν_{max}): 3288, 2962, 1699, 1610, 1485, 1381,1211,1072 cm^{-1}; ^{1}H NMR (300 MHz, DMSO-d_6): δ_H: 0.84 (3H, s, CH_3), 1.00 (3H, s, CH_3), 1.13 (3H, t, J = 7.1 Hz, CH_3), 2.14–2.50 (4H, m, CH_2), 3.97 (2H, q, J = 7.1 Hz, CH_2), 4.84 (1H, s, CH), 7.03–7.20 (5H, m, H_{Ar}), 9.07 (1H, s, NH) ppm. Anal. Calcd for $C_{21}H_{25}NO_3$: C, 74.31; H, 7.42; N, 4.13. Found C, 74.63; H, 7.67; N, 4.27.

6f: IR (KBr) (ν_{max}): 3280, 3217, 3065, 2951, 1695, 1637, 1608, 1489, 1381, 1263, 1210, 1092 cm^{-1}; ^{1}H NMR (300 MHz, DMSO-d_6): δ_H: 0.82 (3H, s, CH_3), 1.00 (3H, s, CH_3), 1.12 (3H, t, J = 7.0 Hz, CH_3), 1.94–2.44 (4H, m, CH_2), 2.29 (3H, s, CH_3), 3.96 (2H, q, J = 7.0 Hz, CH_2), 4.82 (1H, s, CH), 7.08–7.39 (4H, m, H_{Ar}), 9.12 (1H, s, NH) ppm. Anal. Calcd for $C_{21}H_{24}BrNO_3$: C, 60.29; H, 5.78; N, 3.35. Found C, 60.47; H, 5.93; N, 3.47.

7a: IR (KBr) (ν_{max}): 3393, 3317, 3185, 2958, 2196, 1687, 1652, 1367 cm^{-1}. ^{1}H NMR (300 MHz, DMSO–d_6) δ_H: 0.94 (3H, s, CH_3), 1.04 (3H, s, CH_3), 2.08 (1H, d, J = 16.0 Hz, H(CH_2)), 2.23 (1H, d, J = 16.0 Hz, H(CH_2)), 2.50 (2H, m, CH_2), 4.11 (1H, s, CH), 7.06 (2H, br s, NH_2), 7.19 (3H, m, H_{Ar}), 7.33 (2H, m, H_{Ar}) ppm. Anal. Calcd for $C_{18}H_{18}N_2O_2$: C, 73.45; H, 6.16; N, 9.52. Found C, 73.83; H, 6.43; N, 9.41.

7d: IR (KBr) (ν_{max}): 3533, 3364, 3153, 2966, 2193, 1685, 1658, 1367 cm^{-1}. ^{1}H NMR (300 MHz, DMSO–d_6) δH: 1.00 (3H, s, CH_3), 1.06 (3H, s, CH_3), 2.11 (1H, d, J = 16.0 Hz, H(CH_2)), 2.27 (1H, d, J = 16.0 Hz, H(CH_2)), 2.47–2.61 (2H, m, CH_2), 4.70 (1H, s, CH), 7.15 (2H, br s, NH_2), 7.25 (1H, d, J = 8.4 Hz, H_{Ar}), 7.39 (1H, d, J = 8.4 Hz, H_{Ar}), 7.56 (1H, s, H_{Ar}) ppm. Anal. Calcd for $C_{18}H_{16}Cl_2N_2O_2$: C, 59.52; H, 4.44; N, 7.71. Found C, 59.81; H, 4.58; N, 7.61.

RESULTS AND DISCUSSION

Preparation and characterization of the catalyst

The magnetic nanoparticle supported bis sulfamic acid catalyst (MNPs-TBSA) was prepared via sequential reactions as shown in Fig. 2. Magnetite (Fe_3O_4) nanoparticles were easily prepared via the chemical co-precipitation of Fe^{2+} and Fe^{3+} ions in basic solution. These were subsequently coated with silica layer (Fe_3O_4@SiO_2) through the well-known Stober method [48]. The Fe_3O_4@SiO_2 core-shell structures were treated with 3-aminopropyltriethoxysilane (APTS), which can bind covalently to the free-OH groups at the particles surface (Fe_3O_4@SiO_2-NH_2). Triazine-functionalized silica-coated magnetite

nanoparticles (MNPs-TDCl) prepared with the reaction of the 3-aminopropyl-functionalized silica-coated magnetic nanoparticles (Fe_3O_4@SiO_2-NH_2) and triazine trichloride. Reaction of the Triazine-functionalized silica-coated magnetite nanoparticles with ammonia gives the triazine diamine-functionalized silica-coated Fe_3O_4 nanoparticles (Fe_3O_4@SiO_2-TDA). The supported bis-sulfamic acid catalyst (MNPs–TBSA) was prepared via the reaction of MNPs-TDA with chlorosulfonic acid.

The FT-IR spectrum of Fe_3O_4, Fe_3O_4@SiO_2, Fe_3O_4@SiO_2-NH_2, Fe_3O_4@SiO_2-TDCl, Fe_3O_4@SiO_2-TDA and MNPs-TBSA nanoparticles in the wavenumber range of 4000-400 cm^{-1} is shown in Fig. 3. The magnetic Fe_3O_4 nanoparticles FT-IR spectra (Fig. 3a) showed the characteristic Fe–O absorption near 574 cm^{-1}. FT-IR spectrum of Fe_3O_4@SiO_2 displays bands at about 1084 (asymmetric stretching), 951 (symmetric stretching), 808 (in plane bending) and 453 cm^{-1} (rocking mode) of the Si–O–Si group and confirm the formation of SiO_2 shell. The broad peaks in the range 3200–3500 cm^{-1} (stretching vibration mode Si–OH) and the weak peak at 1610 cm^{-1} (twisting vibration mode of H–O–H adsorbed in the silica shell) are obvious in the spectrum. The weak aliphatic vibrations at 2930 and 2955 cm^{-1} (Fig. 3c, d, e and f) related to C–H symmetric and asymmetric stretching and confirmed the presence of the attached alkyl groups. From reaction of cyanuric chloride with Fe_3O_4@SiO_2-NH_2, the peaks correspond to C=N and

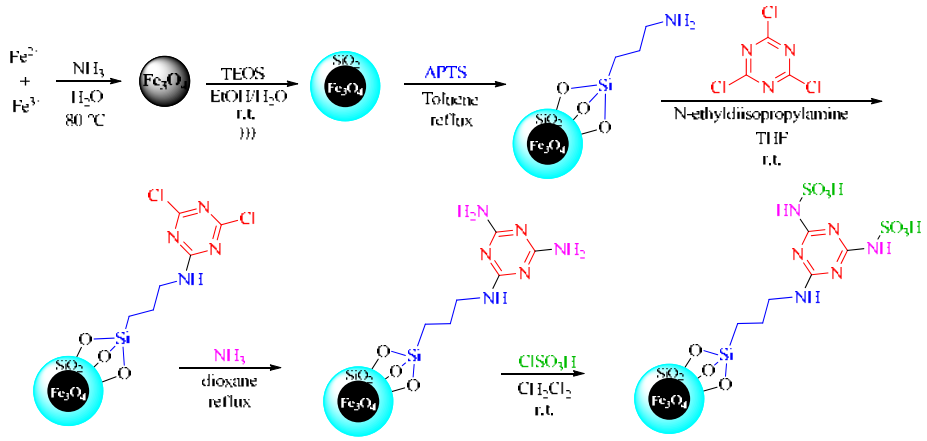

Fig. 2. Preparation of triazinediyl bis sulfamic acid-functionalized silica-coated Fe_3O_4 nanoparticles (MNPs-TBSA).

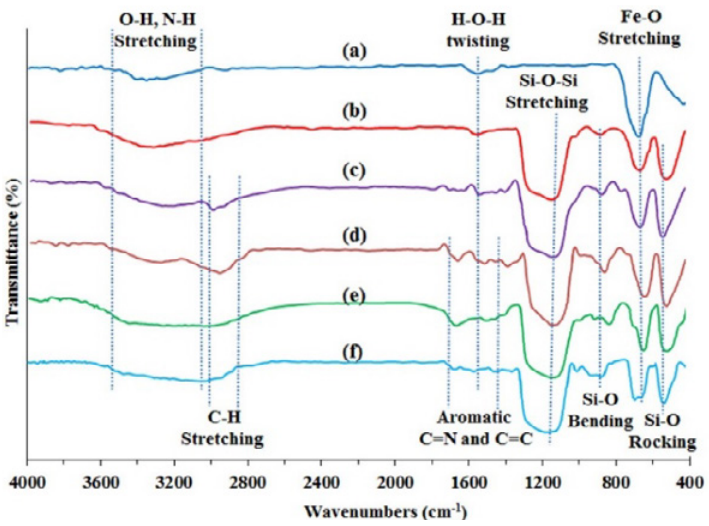

Fig. 3. The comparative FT-IR spectra for (a) Fe_3O_4, (b) Fe_3O_4@SiO_2, (c) Fe_3O_4@SiO_2-NH_2, (d) Fe_3O_4@SiO_2-TDCl, (e) Fe_3O_4@SiO_2-TDA and (d) MNPs-TBSA.

C=C in heterocyclic rings are appeared at 1500-1600 cm^{-1} and 1450 cm^{-1} respectively (Fig. 3d). NH_2 bending of triazine diamine-functionalized MNPs appeared at 1625 cm^{-1} (Fig. 3e) [49]. The peaks at 1400 cm^{-1} have been assigned to the stretching vibrations of S=O acid sulfonic groups. (Fig. 3f) [50]. Therefore the above results prove that the functional groups were successfully grafted on to the surface of the magnetic Fe_3O_4@SiO_2 nanoparticles.

The nanoparticle size and morphology of MNPs-TBSA catalyst were investigated by field emission scanning electron microscopy (FE-SEM) (Fig. 4). As can be seen from Fig. 4, MNPs-TBSA particles have a mean diameter of 25-35 nm and a nearly spherical shape.

In addition, TEM analysis showed a dark nano-Fe_3O_4 core surrounded by a grey silica shell about 5-10 nm thick and the average size of the obtained particles is 20-35 nm (Fig. 5).

The energy dispersive X-ray spectroscopy (EDS) results, obtained from SEM analysis of MNPs- TBSA, are shown in Fig. 6, and clearly show the presence of S in the MNPs-TBSA catalyst. Moreover, the presence of Si, O, and Fe signals indicates that the iron oxide particles are loaded into silica, and the higher intensity of the Si peak compared with the Fe peaks indicates that the Fe_3O_4 nanoparticles were trapped by SiO_2. According to the above analysis, it can be concluded that the MNPs-TBSA have been successfully synthesized.

The presence as well as the degree of crystallinity of magnetic Fe_3O_4 and the MNPs-TBSA catalyst was obtained from XRD measurements (Fig. 7). The same peaks were observed in the both of the magnetic Fe_3O_4 and MNPs-TBSA XRD patterns, indicating retention of the crystalline spinel ferrite core structure during the silica-

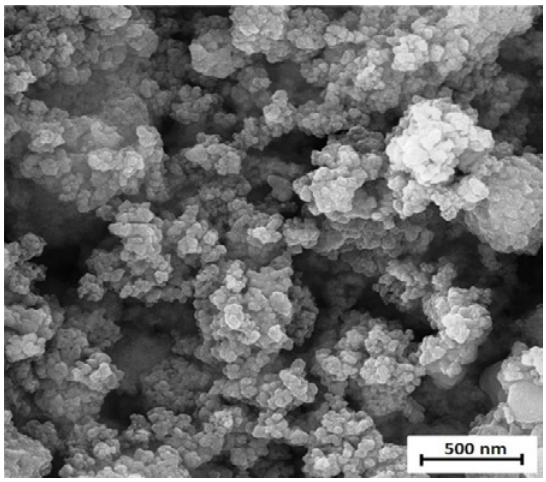

Fig. 4. The FE-SEM images of MNPs–TBSA nanoparticles.

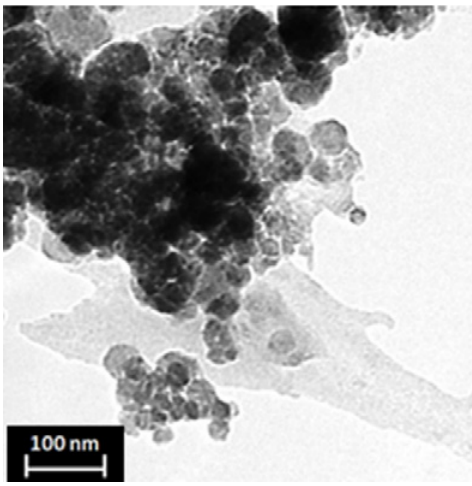

Fig. 5. TEM image of MNPs-TBSA nanoparticles.

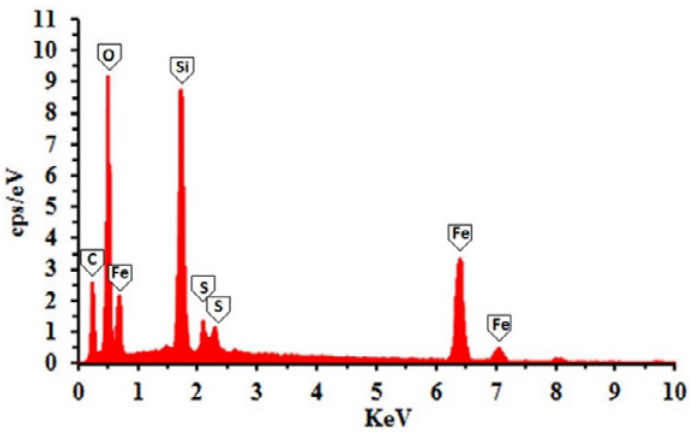

Fig. 6. The EDS spectrum of MNPs-TBSA nanoparticles.

coating process. The XRD data of the synthesized magnetic nanoparticles show diffraction peaks at 2θ = 30.3° ,35.7°, 43.3°, 53.7°, 57.3°, 62.9°, and 74.5° which can be assigned to the (220), (311), (400), (422), (511), (440) and (533) planes of Fe_3O_4, respectively, indicating that the Fe_3O_4 particles in the nanoparticles were pure Fe_3O_4 with a cubic spinel structure; these match well with the standard Fe_3O_4 sample (JCPDS card no. 85-1436). The broad peak from 2θ = 20° to 27 ° (Fig. 5b) is consistent with an amorphous silica phase in the shell of the silica-coated Fe_3O_4 nanoparticles (Fe_3O_4@SiO_2) [51]. The (311) XRD peak was used to estimate the average crystallite size of the magnetic nanoparticles by Scherrer's equation ($D = 0.9\lambda/\beta \cos \theta$), where D is the average crystalline size, λ is the X-ray wave-length (0.154 nm), β denotes the full width in radians subtended by the half maximum intensity width of the (311) powder peak, and θ corresponds to the Bragg angle of the (311) peak in degrees [52]. From the width of the peak at 2θ = 35.7 (311), the crystallite size of the magnetic nanoparticle is calculated to be 15.5 nm using Scherrer's equation, which is in range the size determined by FE-SEM analysis (Fig. 4).

The stability of the MNPs-TBSA catalyst was determined by thermogravimetric analysis (TGA) and derivative thermogravimetry (DTG) (Fig. 8). The magnetic catalyst shows two step weight loss steps over the temperature range of TG analysis. The first stage, including a low amount of weight loss at T< 200 °C, is due to the removal of physically adsorbed solvent and surface hydroxyl groups, the second stage at about 220 °C to nearly 560 °C is attributed to the decomposition of the organic moiety in the nanocomposite. Therefore, the weight loss between 220-560 °C gives the organic grafting ratios of the magnetic catalyst. The grafted organic moiety on the magnetic Fe_3O_4@SiO_2 nanoparticles was approximately 16 wt%. In accordance with this mass loss, it was calculated that 0.40 mmol of TBSA was loaded on 1 g of MNPs-TBSA catalyst. Therefore, the MNPs-TBSA is stable around or below 250 °C. The agreement between the acid amount of MNPs-TBSA (0.35 mmol g^{-1}) measured by back titration using HCl and the

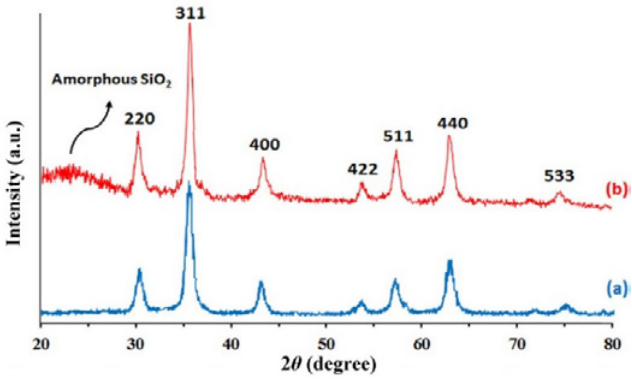

Fig. 7. XRD diffraction pattern of Fe_3O_4 MNPs (a), and MNPs-TBSA (b).

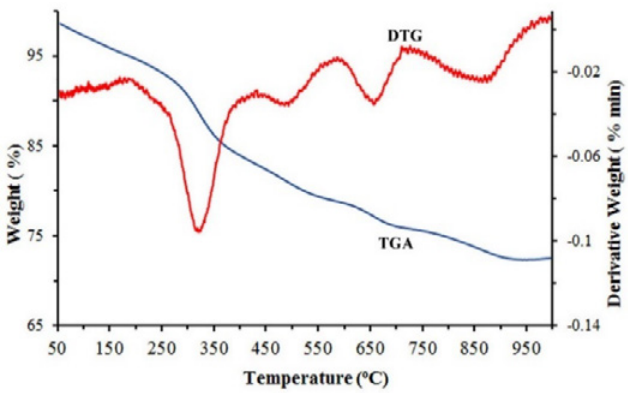

Fig. 8. TG-DTG analyses for MNPs-TBSA nanoparticles.

organic group loading determined by TGA (0.40 mmol g^{-1}), is clear evidence that the triazinediyl bis sulfamic acid groups are principally located on the surfaces of Fe_3O_4@SiO_2 nanoparticles, where they are accessible for adsorption and catalytic reaction processes.

After the characterization of the MNPs-TBSA catalyst, its catalytic activity was evaluated for the synthesis of polyhydroquinoline derivatives (Scheme 1). An important feature of these nano-catalysts is simple separation of them using an external magnet, thereby removing the necessity for filtration or centrifugation. In order to optimize the reaction conditions and obtain the best catalytic activity, the reaction of benzaldehyde, dimedone, ethylacetoacetate and ammonium acetate was used as a model, and was conducted under different reaction parameters (Table 1). As shown in Table 1 (entry 7), the best result was found in EtOH at 70 °C using 30 mg of the catalyst. Moreover, the catalyst is essential and in the absence of the catalyst, only 23% of the corresponding polyhydroquinoline was produced even after prolonged reaction times (Table 1, entry 10). The efficiencies of Fe_3O_4, Fe_3O_4@SiO_2 and MNPs-NH_2, Fe_3O_4@SiO_2-TDA and MNPs-TBSA as the catalyst towards the model reaction were compared and the results are depicted in Table

Table 1. Optimization of reaction conditions for preparation of polyhydroquinolines

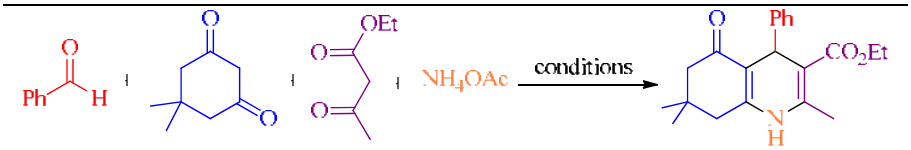

No.	Catalyst (mg)	Solvent	Temp. (°C)	Time (min)	Yield (%) [a]
1	MNPs-TBSA (20)	CH_3CN	Reflux	45	67
2	MNPs-TBSA (20)	$CHCl_3$	Reflux	45	42
3	MNPs-TBSA (20)	THF	Reflux	30	71
4	MNPs-TBSA (20)	H_2O	Reflux	45	53
5	MNPs-TBSA (20)	EtOH	Reflux	25	81
6	MNPs-TBSA (30)	EtOH	Reflux	25	93
7	MNPs-TBSA (30)	EtOH	70 °C	25	95
8	MNPs-TBSA (30)	EtOH	50	25	83
9	MNPs-TBSA (30)	EtOH	r.t.	25	51
10	-	EtOH	Reflux	90	23
11	Fe_3O_4 (30)	EtOH	Reflux	30	41
12	Fe_3O_4@SiO_2 (30)	EtOH	Reflux	30	48
13	MNPs-NH_2 (30)	EtOH	Reflux	30	43
14	MNPs-TDA (30)	EtOH	Reflux	30	47

[a] Isolated yields.

Table 2. Multicomponent one-pot synthesis of polyhydroquinolines catalyzed by MNPs-TBSA

Product	Ar	Time (min)	Yield (%)[a]	MP (°C)[b]	
				Found	Reported
6a	C_6H_5	25	95	204-205	202-204[26b]
6b	2-NO_2-C_6H_4	25	92	204-206	206-207[26a]
6c	3-NO_2-C_6H_4	25	90	179-181	178-179[26a]
6d	4-NO_2-C_6H_4	25	96	240-242	243-244[26a]
6e	4-Cl-C_6H_4	25	93	242-244	245-246[26a]
6f	4-Br-C_6H_4	30	91	252-253	253-255[26b]
6g	4-CH_3-C_6H_4	30	93	260-262	260-261[26b]
6h	4-OH-C_6H_4	30	91	232-233	230-231[26a]
6i	4-OMe-C_6H_4	30	92	253-255	255-257[26a]
6j	4-$N(Me)_2$-C_6H_4	30	91	259-261	262-263[26a]
6k	3-OH-C_6H_4	30	90	230-232	236-238[26a]
6l	2-Cl-C_6H_4	25	89	204-205	207-208[26a]
6m	2,4-Cl_2-C_6H_3	30	93	240-241	241-243[26b]
6n	3,4-(OCH_3)-C_6H_3	20	90	202-203	198-199[26a]
6o	C_6H_5-CH=CH-	25	86	199-201	204-206[26b]

[a] Isolated yields
[b] Melting points were not corrected

1. It was observed that the MNPs-TBSA was more efficient than the other ones (entries 7-14). In order to determine the generality and efficacy of the catalyst, various aldehyde carrying either electron-donating or electron-withdrawing groups were reacted under the optimized reaction condition (Table 2). All reactions proceeded efficiently in the presence of catalytic amounts of MNPs-TBSA at 70 °C and the desired products were obtained in good to excellent yields (86–96%) in relatively short reaction times, without formation of side products.

A plausible mechanism for the formation of polyhydroquinolines catalyzed by MNPs-TBSA, is shown in Fig. 9. The MNPs-TBSA catalyst participates in the reaction by activating the carbonyl group of the aldehyde followed by the nucleophilic addition of dimedone anion and H_2O elimination to obtain alkene intermediate. The alkene intermediate is attacked by enolized ethyl acetoacetate. This intermediate reacts with ammonium acetate and an intramolecular cyclization and H_2O elimination afford the desired polyhydroquinoline.

To compare the applicability of our catalyst with other catalysts used for the synthesis of polyhydroquinoline derivatives, the results of these catalysts in the condensation reaction of benzaldehyde, ethylacetoacetate, dimedone and ammonium acetate under optimized conditions have been indicated in Table 3. As can be seen, the catalytic system reported in this paper has benefits in terms of simple conditions, short reaction times and excellent yields and is superior to many other methods.

Encouraged by the obtained results on polyhydroquinolines preparation, the possible synthesis of tetrahydrobenzopyrans was examined in the presence of MNPs-TBSA as a catalyst in the same conditions. Ethanol serves as the best solvent with respect to green nature, polarity and clean workup procedure for this synthesis. For the reaction completion, 30 mg of the catalyst (MNPs-TBSA) is sufficient. Likewise, arylaldehydes with either electron-withdrawing or electrondonating groups were examined using the optimized conditions to afford a wide range of desired 4*H*-benzo[*b*]pyran in good to excellent yields (85-95%) in short reaction times (Table 4).

Catalyst recovery and reuse

The recovery and reusability of the catalyst are very important for commercial and industrial applications as well as green process aspects.

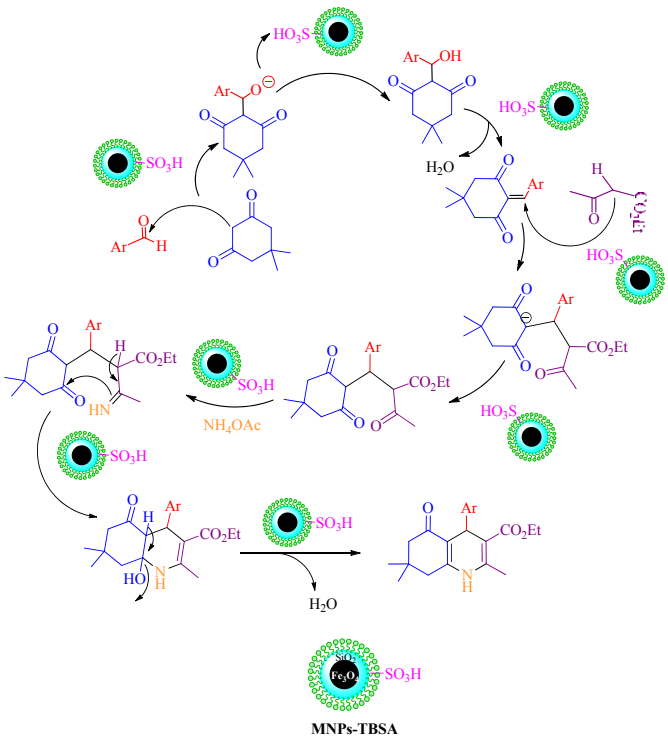

Fig. 9. The proposed mechanism for polyhydroqinoline synthesis using MNPs-TBSA catalyst

Table 3. Comparison of MNPs-TBSA with some other catalysts described in the literature for the synthesis of polyhydroquinolines[a]

Entry	Catalyst	Condition	Time (min)	Yield (%)[b]	Ref.
1	$[hmim]BF_4$	Solvent-free, 90 ºC	10	95	[19]
2	L-proline	EtOH, rt	120	85	[21]
3	I_2	Solvent-free, rt	90	93	[26a]
4	CAN	Solvent-free, rt	60	92	[26b]
5	$Yb(OTf)_3$	EtOH, rt	300	90	[27]
6	MNPs@GSA	EtOH, reflux	240	90	[28a]
7	TritonX-100	H_2O, rt	90	94	[28b]
8	$Sc(OTf)_3$	EtOH, rt	240	93	[28c]
9	$Hf(NPf_2)_4$	$C_{10}F_{18}$, 60 ºC	180	95	[28d]
10	MNPs-TBSA	EtOH, 70 ºC	25	95	Present work

[a] Reaction conditions: benzaldehyde (1 mmol), ethylacetoacetate (1 mmol), dimedone (1 mmol), ammonium acetate (1.2 mmol).
[b] Isolated yields.

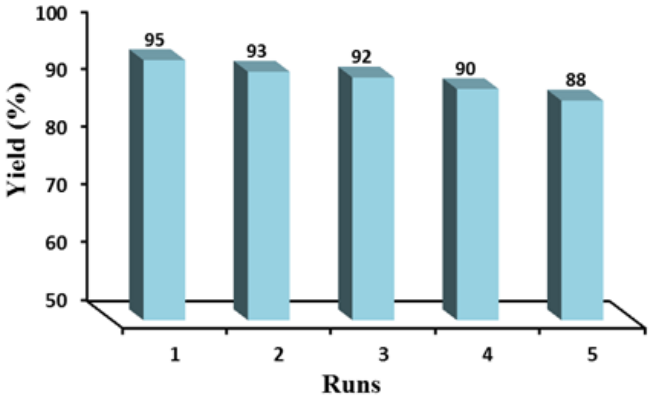

Fig. 10. Recyclability of MNPs-TBSA in the preparation of polyhydroquinolines in EtOH at 70 °C.

Table 4. Multicomponent one-pot synthesis of 4*H*-benzo[*b*]pyrans catalyzed by MNPs-TBSA

Product	Ar	Time (min)	Yield (%)[a]	MP (°C)[b]	
				Found	Reported
7a	C_6H_5	25	95	227-228	228-230[36]
7b	$3\text{-}Cl\text{-}C_6H_4$	25	94	225-227	224-225[36]
7c	$4\text{-}Cl\text{-}C_6H_4$	25	90	213-214	209-211[36]
7d	$2,4\text{-}Cl_2\text{-}C_6H_3$	25	95	183-185	180-182[34b]
7e	$4\text{-}Br\text{-}C_6H_4$	25	89	200-202	203-205[30]
7f	$3\text{-}OH\text{-}C_6H_4$	30	91	233-235	236-238[34a]
7g	$4\text{-}OH\text{-}C_6H_4$	30	93	205-207	206-208[34a]
7h	$2\text{-}NO_2\text{-}C_6H_4$	30	86	225-227	224-226[30]
7i	$3\text{-}NO_2\text{-}C_6H_4$	30	89	161-163	212-214[30]
7j	$4\text{-}NO_2\text{-}C_6H_4$	30	91	177-179	177-178[30]
7k	$4\text{-}CH_3\text{-}C_6H_4$	30	90	163-166	223-225[34a]
7l	$4\text{-}N(Me)_2\text{-}C_6H_4$	30	89	213-215	230[33]
7m	$4\text{-}OCH_3\text{-}C_6H_4$	25	90	126-128	203[33]

[a] Isolated yields
[b] Melting points were not corrected

Thus, the recovery and reusability of MNPs-TBSA (30 mg) was investigated in the sequential reaction of benzaldehdye (1 mmol) with other reactants and MNPs-TBSA (30 mg) as catalyst in EtOH at 70 °C for 25 min. After completion of the reaction, the resulting solidified mixture was diluted with hot EtOH (15 mL). Then, the catalyst was easily separated using an external magnet, washed

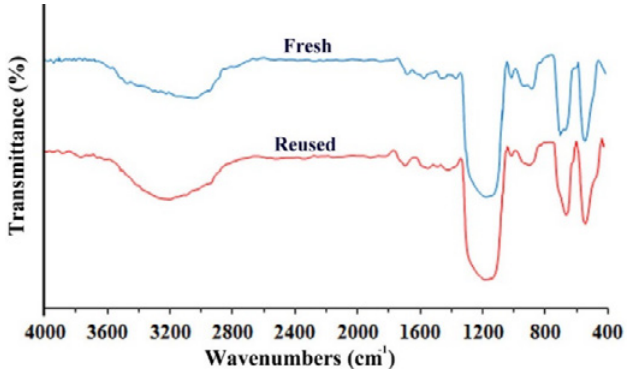

Fig. 11. FT-IR spectra of the fresh catalyst and the five-times reused catalyst.

with hot EtOH, dried under vacuum and reused in a subsequent reaction. Nearly quantitative recovery of catalyst (up to 98%) could be obtained from each run. As seen in Fig. 10, the recycled catalyst could be reused five times without any additional treatment or appreciable reduction in catalytic activity. The recovered catalyst after five runs had no obvious change in structure, as shown by comparison of the FT-IR spectra to that of fresh catalyst (Fig. 11). The consistent structure and activity of recovered and reused MNPs-TBSA catalyst indicates that the reused MNPs-TBSA also shows excellent performance for the synthesis of desired heterocycles.

CONCLUSION

In conclusion, we have described a successful preparation of bissulfamic acid-functionalized magnetic nanoparticles as an efficient, magnetically separable and reusable heterogeneous catalyst. We have considered also convenient synthesis of polyhydroquinoline and 4*H*-benzo[*b*]pyran derivatives via one-pot multicomponent reaction in the presence of prepared catalyst on green reaction condition. The method offers several advantages including mild reaction condition, simple work-up procedure, recyclability of catalyst, high purity of products, excellent yields and short reaction time.

ACKNOWLEDGEMENTS

We gratefully acknowledge the financial support of this work by the research council of Arak University.

CONFLICT OF INTERESTS

The authors declare that there is no conflict of interests regarding the publication of this paper.

REFERENCES

1. Ghanta Mahesh R, Mehendra S, Akula Kalyan C. Chemical and Pharmacological Significance of 1,4-Dihydropyridines. Current Organic Chemistry. 2007;11(10):847-52.
2. Auterhoff H. Textbook of Organic Medicinal and Pharmaceutical Chemistry. Herausgegeben von Ch.O. Wilson, O. Gisvold und R.G. Doerge. 6. Auflage, 1053 Seiten. J.B. Lippincott Co, Philadelphia and Toronto, und Blackwell Scientific Publications, Oxford and Edinburgh 1971. Preis: £ 12.00. Archiv der Pharmazie. 1972;305(4):316-.
3. Briede J, Daija D, Stivrina M, Duburs G. Effect of cerebrocrast on the lymphocyte blast transformation activity in normal and streptozotocin-induced diabetic rats. Cell Biochemistry and Function. 1999;17(2):89-96.
4. Bird GLA, Prach AT, McMahon AD, Forrest JAH, Mills PR, Danesh BJ. Randomised controlled double-blind trial of the calcium channel antagonist amlodipine in the treatment of acute alcoholic hepatitis. Journal of Hepatology. 1998;28(2):194-8.
5. Buhler FR, Kiowski W. Calcium Antagonists in Hypertension. Journal of Hypertension. 1987;5(3):S3???10.
6. Safak C, Simsek R. Fused 1,4-Dihydropyridines as Potential Calcium Modulatory Compounds. Mini-Reviews in Medicinal Chemistry. 2006;6(7):747-55.
7. Brahmachari G. Green Synthetic Approaches for Biologically Relevant Heterocycles. Green Synthetic Approaches for Biologically Relevant Heterocycles: Elsevier; 2015. p. 1-6.
8. Wu JY-C, Fong W-F, Zhang J-X, Leung C-H, Kwong H-L, Yang M-S, et al. Reversal of multidrug resistance in cancer cells by pyranocoumarins isolated from Radix Peucedani. European Journal of Pharmacology. 2003;473(1):9-17.
9. Rueping M, Sugiono E, Merino E. Asymmetric Organocatalysis: An Efficient Enantioselective Access to Benzopyranes and Chromenes. Chemistry - A European Journal. 2008;14(21):6329-32.
10. Moon D-O, Kim K-C, Jin C-Y, Han M-H, Park C, Lee K-J, et al. Inhibitory effects of eicosapentaenoic acid on lipopolysaccharide-induced activation in BV2 microglia. International Immunopharmacology. 2007;7(2):222-9.
11. Morgan LR, Jursic BS, Hooper CL, Neumann DM, Thangaraj K, LeBlanc B. Anticancer activity for 4,4′-Dihydroxybenzophenone-2,4-dinitrophenylhydrazone (A-007) analogues and Their abilities to interact with lymphoendothelial cell surface markers. Bioorganic & Medicinal Chemistry Letters. 2002;12(23):3407-11.

12. Pérez-Sacau E, Estévez-Braun A, Ravelo ÁG, Gutiérrez Yapu D, Giménez Turba A. Antiplasmodial Activity of Naphthoquinones Related to Lapachol andβ-Lapachone. Chemistry & Biodiversity. 2005;2(2):264-74.
13. Kumar A, Maurya RA, Sharma S, Ahmad P, Singh AB, Bhatia G, et al. Pyranocoumarins: A new class of anti-hyperglycemic and anti-dyslipidemic agents. Bioorganic & Medicinal Chemistry Letters. 2009;19(22):6447-51.
14. Hantzsch A. Ueber die Synthese pyridinartiger Verbindungen aus Acetessigäther und Aldehydammoniak. Justus Liebig's Annalen der Chemie. 1882;215(1):1-82.
15. Simon Cl, Constantieux T, Rodriguez J. Utilisation of 1,3-Dicarbonyl Derivatives in Multicomponent Reactions. European Journal of Organic Chemistry. 2004;2004(24):4957-80.
16. Dondoni A, Massi A, Minghini E, Bertolasi V. Multicomponent Hantzsch cyclocondensation as a route to highly functionalized 2- and 4-dihydropyridylalanines, 2- and 4-pyridylalanines, and their N-oxides: preparation via a polymer-assisted solution-phase approach. Tetrahedron. 2004;60(10):2311-26.
17. Shestopalov AM, Emelianova YM, Nesterov VN. Russ Chem Bull. 2003;52(5):1164-1171.
18. Wan J-P, Liu Y. Recent advances in new multicomponent synthesis of structurally diversified 1,4-dihydropyridines. RSC Advances. 2012;2(26):9763.
19. Ji S-J, Loh T-P, Jiang Z-Q, Lu J. Facile Ionic Liquids-Promoted One-Pot Synthesis of PolyhydroquinolineDerivatives under Solvent Free Conditions. Synlett. 2004(5):0831-5.
20. Li M, Guo W-S, Wen L-R, Li Y-F, Yang H-Z. One-pot synthesis of Biginelli and Hantzsch products catalyzed by non-toxic ionic liquid (BMImSac) and structural determination of two products. Journal of Molecular Catalysis A: Chemical. 2006;258(1-2):133-8.
21. Kumar A, Maurya RA. Synthesis of polyhydroquinoline derivatives through unsymmetric Hantzsch reaction using organocatalysts. Tetrahedron. 2007;63(9):1946-52.
22. Sridhar R, Perumal PT. A new protocol to synthesize 1,4-dihydropyridines by using 3,4,5-trifluorobenzeneboronic acid as a catalyst in ionic liquid: synthesis of novel 4-(3-carboxyl-1H-pyrazol-4-yl)-1,4-dihydropyridines. Tetrahedron. 2005;61(9):2465-70.
23. Safari J, Banitaba SH, Khalili SD. Cellulose sulfuric acid catalyzed multicomponent reaction for efficient synthesis of 1,4-dihydropyridines via unsymmetrical Hantzsch reaction in aqueous media. Journal of Molecular Catalysis A: Chemical. 2011;335(1-2):46-50.
24. Tamaddon F, Moradi S. Controllable selectivity in Biginelli and Hantzsch reactions using nanoZnO as a structure base catalyst. Journal of Molecular Catalysis A: Chemical. 2013;370:117-22.
25. Sabitha G, Reddy GSKK, Reddy CS, Yadav JS. A novel TMSI-mediated synthesis of Hantzsch 1,4-dihydropyridines at ambient temperature. Tetrahedron Letters. 2003;44(21):4129-31.
26. Ko S, Sastry MNV, Lin C, Yao C-F. Molecular iodine-catalyzed one-pot synthesis of 4-substituted-1,4-dihydropyridine derivatives via Hantzsch reaction. Tetrahedron Letters. 2005;46(34):5771-4.
27. Wang L-M, Sheng J, Zhang L, Han J-W, Fan Z-Y, Tian H, et al. Facile Yb(OTf)3 promoted one-pot synthesis of polyhydroquinoline derivatives through Hantzsch reaction. Tetrahedron. 2005;61(6):1539-43.
28. Poor Heravi MR, Mehranfar S, Shabani N. One-pot multicomponent synthesis hexahydroquinoline derivatives in Triton X-100 aqueous micellar media. Comptes Rendus Chimie. 2014;17(2):141-5.
29. Li JT, Xu WZ, Yang LC, Li TS. One-Pot Synthesis of 2-Amino-4-aryl-3-carbalkoxy-7,7-dimethyl-5,6,7,8-tetrahydrobenzo[b]pyran Derivatives Catalyzed by KF/Basic Al2O3Under Ultrasound Irradiation. Synthetic Communications. 2004;34(24):4565-71.
30. Jin T-S, Zhang J-S, Xiao J-C, Wang A-Q, Li T-S. Clean Synthesis of 1,8-Dioxo-octahydroxanthene Derivatives Catalyzed byp-Dodecylbenezenesulfonic Acid in Aqueous Media. Synlett. 2004(5):0866-70.
31. Shi DQ, Zhang S, Zhuang QY, Tu SJ, Hu HW. Clean synthesis of 2-amino-3-cyano-4-aryl-7, 7-dimethyl-5-oxo-4H-5, 6, 7, 8-tetrahydrobenzo [b] pyran in water. Chinese Journal of Organic Chemistry. 2003;23(8):877-879.
32. Peng Y, Song G. Amino-functionalized ionic liquid as catalytically active solvent for microwave-assisted synthesis of 4H-pyrans. Catalysis Communications. 2007;8(2):111-4.
33. Hekmatshoar R, Majedi S, Bakhtiari K. Sodium selenate catalyzed simple and efficient synthesis of tetrahydro benzo[b]pyran derivatives. Catalysis Communications. 2008;9(2):307-10.
34. Balalaie S, Bararjanian M, Amani AM, Movassagh B. (S)-Proline as a Neutral and Efficient Catalyst for the One-Pot Synthesis of Tetrahydrobenzo[b]pyran Derivatives in Aqueous Media. ChemInform. 2006;37(23).
35. Lian X-Z, Huang Y, Li Y-Q, Zheng W-J. A Green Synthesis of Tetrahydrobenzo[b]pyran Derivatives through Three-Component Condensation Using N-Methylimidazole as Organocatalyst. Monatshefte für Chemie - Chemical Monthly. 2007;139(2):129-31.
36. Tu S-J, Gao Y, Guo C, Shi D, Lu Z. A CONVENIENT SYNTHESIS OF 2-AMINO-5,6,7,8-TETRAHYDRO-5-OXO- 4-ARYL-7,7-DIMETHYL-4H-BENZO-[b]-PYRAN-3-CARBONITRILE UNDER MICROWAVE IRRADIATION. Synthetic Communications. 2002;32(14):2137-41.
37. Sharma N, Ojha H, Bharadwaj A, Pathak DP, Sharma RK. Preparation and catalytic applications of nanomaterials: a review. RSC Advances. 2015;5(66):53381-403.
38. Mortazavi-Derazkola S, Zinatloo-Ajabshir S, Salavati-Niasari M. New sodium dodecyl sulfate-assisted preparation of Nd2O3 nanostructures via a simple route. RSC Advances. 2015;5(70):56666-76.
39. Han L, Choi H-J, Choi S-J, Liu B, Park D-W. Ionic liquids containing carboxyl acid moieties grafted onto silica: Synthesis and application as heterogeneous catalysts for cycloaddition reactions of epoxide and carbon dioxide. Green Chemistry. 2011;13(4):1023.
40. Nasseri MA, Sadeghzadeh M. Multi-component reaction on free nano-SiO2 catalyst: Excellent reactivity combined with facile catalyst recovery and recyclability. Journal of Chemical Sciences. 2013;125(3):537-44.
41. Polshettiwar V, Luque R, Fihri A, Zhu H, Bouhrara M, Basset J-M. Magnetically Recoverable Nanocatalysts. Chemical Reviews. 2011;111(5):3036-75.
42. Morel A-L, Nikitenko SI, Gionnet K, Wattiaux A, Lai-Kee-Him J, Labrugere C, et al. Sonochemical Approach to the Synthesis of Fe3O4@SiO2 Core–Shell Nanoparticles with Tunable Properties. ACS Nano. 2008;2(5):847-56.
43. Mobinikhaledi A, Moghanian H, Sasani F. A Simple and Convenient Method for the Synthesis of Perimidine

Derivatives Catalyzed by Nano-Silica Sulfuric Acid. International Journal of Green Nanotechnology: Physics and Chemistry. 2010;2(2):P47-P52.
44. Bodaghifard MA, Ahadi N. Sulfamic acid: A green and efficient catalyst for synthesis of mono-, bis-, and spiro-perimidines. Iranian Journal of Catalysis. 2016;6(4):377-380.
45. Bodaghifard MA, Solimannejad M, Asadbegi S, Dolatabadifarahani S. Mild and green synthesis of tetrahydrobenzopyran, pyranopyrimidinone and polyhydroquinoline derivatives and DFT study on product structures. Research on Chemical Intermediates. 2015;42(2):1165-79.
46. Bodaghifard MA, Asadbegi S, Bahrami Z. (Triazinediyl) bis sulfamic acid-functionalized silica-coated magnetite nanoparticles: Preparation, characterization and application as an efficient catalyst for synthesis of mono-, bis-, tris- and spiro-perimidines. Journal of the Iranian Chemical Society. 2016;14(2):365-76.
47. Bodaghifard MA, Mobinikhaledi A, Asadbegi S. Bis(4-pyridylamino)triazine-stabilized magnetite nanoparticles: preparation, characterization and application as a retrievable catalyst for the green synthesis of 4H-pyran, 4H-thiopyran and 1,4-dihydropyridine derivatives. Applied Organometallic Chemistry. 2016;31(2):e3557.
48. Stöber W, Fink A, Bohn E. Controlled growth of monodisperse silica spheres in the micron size range. Journal of Colloid and Interface Science. 1968;26(1):62-9.
49. Marchewka MK. Infrared and Raman spectra of melaminium chloride hemihydrate. Materials Science and Engineering: B. 2002;95(3):214-21.
50. Buzzoni R, Bordiga S, Ricchiardi G, Spoto G, Zecchina A. Interaction of H2O, CH3OH, (CH3)2O, CH3CN, and Pyridine with the Superacid Perfluorosulfonic Membrane Nafion: An IR and Raman Study. The Journal of Physical Chemistry. 1995;99(31):11937-51.
51. Feng G, Hu D, Yang L, Cui Y, Cui X-a, Li H. Immobilized-metal affinity chromatography adsorbent with paramagnetism and its application in purification of histidine-tagged proteins. Separation and Purification Technology. 2010;74(2):253-60.
52. Giri J, Guha Thakurta S, Bellare J, Kumar Nigam A, Bahadur D. Preparation and characterization of phospholipid stabilized uniform sized magnetite nanoparticles. Journal of Magnetism and Magnetic Materials. 2005;293(1):62-8.